A024
Dual Porosity Biot-Barenblatt Model

G.M. Goloshubin* (University of Houston) & D.B. Silin (University of California)

SUMMARY

Dual porosity Biot-Barenblatt poroelastic model is analyzed. P-wave reflection at an impermeable interface between elastic and dual-porosity media is investigated. Asymptotic low-frequency analysis of the planar p-wave reflection coefficient from a hydrocarbon reservoir shows that the frequency-dependent component is proportional to the square root of the reservoir fluid mobility. Frequency-dependent seismic attribute analysis has been applied for mapping of high fluid mobility zones of oil-saturated reservoirs. As the obtained asymptotic scaling links reservoir rock and fluid properties with seismic attributes, it has a great potential for hydrocarbon exploration and production.

Introduction

The fundamental theory of elastic wave propagation in a fluid-saturated porous rock has been developed by Biot (1956ab). Wave propagation in rocks with two scales of permeability was analyzed by Pride and Berryman (2003ab). The classical model of fractured reservoir developed in petroleum engineering literature (Barenblatt *et al.*, 1960, Warren and Root, 1963) is employed. According to this model, the porous medium can be presented as a superposition of two media. Both of them are presented in every representation elementary volume. One medium, fractures, supports the transport properties of the rock, whereas the other one, matrix, provides the volume where the fluid is stored. The matrix permeability is low relative to that of the fractures and the flow between matrix blocks can be carried out through the fractures only. We have developed asymptotic analysis of the reflection coefficient from the dual medium in the low-frequency range of seismic spectrum taking into account both Biot's poroelasticity and Barenblatt's dual medium. We use Biot-Barenblatt model for frequency-dependent attribute analysis of seismic data to map oil-saturated reservoir zones with high permeability.

Governing Equation

We have obtained the governing equations in a dimensionless form and use $\varepsilon = i\dfrac{\rho_f \kappa \omega}{\eta}$ as the small dimensionless parameter in our asymptotic analysis. Here ρ_f is the density of reservoir fluid, κ is reservoir rock permeability, η is fluid viscosity, ω is the angular frequency of the signal and i is the imaginary unity. Below are an asymptotic analysis of a harmonic-wave solution to the governing equations and a simple expression of the planar p-wave reflection coefficient.

Denote by u the skeleton displacement, W Darcy fluid velocity and p fluid pressure. Then, from the basic principles of filtration theory and linear elasticity, one obtains

$$\begin{aligned}
\frac{\partial^2 u}{\partial t^2} + \gamma_\rho \frac{\partial W}{\partial t} &= v_b^2 \frac{\partial^2 u}{\partial x^2} - v_f^2 \frac{\partial P}{\partial x} \\
\rho_f \frac{\kappa}{\eta}\frac{\partial^2 u}{\partial t^2} + W + \tau \frac{\partial W}{\partial t} &= -D\frac{\partial P}{\partial x} \qquad (1)\\
\frac{\partial^2 u}{\partial t \partial x} + \frac{\partial P}{\partial t} &= -\frac{\partial W}{\partial x}
\end{aligned}$$

Here t is time and x is the coordinate aligned with wave propagation; γ_ρ is the ratio of fluid density ρ_f to the saturated-medium bulk density ρ_b, $D = \dfrac{\kappa}{\phi \eta \beta_f}$ is the hydraulic diffusivity, where ϕ is the reservoir rock porosity and β_f is adiabatic fluid compressibility. Velocities v_b and v_f are defined as

$$v_f^2 = \frac{1}{\beta \rho_b} \qquad \text{and} \qquad v_b^2 = \frac{1}{\phi \beta_f \rho_b} \qquad (2)$$

We seek a solution to system of equations (1) in the form of harmonic plane wave

$$u = U_0 e^{i(\omega t - kx)}, \quad W = W_0 e^{i(\omega t - kx)}, \quad P = P_0 e^{i(\omega t - kx)} \ (3)$$

where k is a complex wave number yet to be determined. For asymptotic analysis, the following dimensionless variables are introduced

$$\varsigma = \frac{\omega^2}{k^2 v_f^2}, \quad \xi = -i\frac{P_0}{kU_0}, \quad \chi = i\frac{W_0}{\omega U_0} \qquad (4)$$

Then, equations (1) take on the following dimensionless form

$$\begin{aligned} -\varsigma + \xi + \gamma_\rho \varsigma\xi &= -\gamma_v \\ \varepsilon\left(-\varsigma + \frac{1}{\gamma_\rho}\xi + \theta\varsigma\chi\right) + \varsigma\chi &= 0 \qquad (5) \\ \xi + \chi &= 1 \end{aligned}$$

Where $\gamma_v = \frac{\phi\beta_f}{\beta}$ and $\theta = \frac{\eta\tau}{\rho_f \kappa}$. In this study, we assume that $\theta = O(1)$. We seek an asymptotic solution as power series with respect to the small parameter ε:

$$\begin{aligned} \varsigma &= \varsigma_0 + \varsigma_1\varepsilon + o(\varepsilon), \\ \xi &= \xi_0 + \xi_1\varepsilon + o(\varepsilon), \qquad (6) \\ \chi &= \chi_0 + \chi_1\varepsilon + o(\varepsilon) \end{aligned}$$

Two solutions corresponding to slow and fast wave are

$$\begin{aligned} \varsigma_0^S &= 0 & \varsigma_1^S &= \gamma_v\delta \\ \xi_0^S &= -\gamma_v & \xi_1^S &= \gamma_v(\delta - 1) \qquad (7) \\ \chi_0^S &= 1 + \gamma_v & \chi_1^S &= \gamma_v(1 - \delta) \end{aligned}$$

$$\begin{aligned} \varsigma_0^F &= 1 + \gamma_v & \varsigma_1^F &= \delta + \frac{1}{\delta} - 2 \\ \xi_0^F &= 1 & \xi_1^F &= \delta - 1 \qquad (8) \\ \chi_0^S &= 0 & \chi_1^F &= 1 - \delta \end{aligned}$$

Where $\delta = \frac{1}{\gamma_\rho(1+\gamma_v)}$. Note that all coefficients in Equations (7)-(8) are real. Equations (4) and (7)-(8), in particular, imply that the slow wave propagates in the fluid, whereas the fast wave does not involve the fluid motion. In addition, the first asymptotic terms of the wave number and attenuation factor of the slow wave are equal to each other and asymptotically proportional to $\sqrt{\omega}$:

$$a^S \approx k^S = \frac{\omega}{v_b\sqrt{2\delta|\varepsilon|}} + \omega O\left(|\varepsilon|^{1/2}\right) \qquad (9)$$

For the fast wave, the wave number and attenuation factor asymptotic expressions are

$$k^F = \frac{\omega}{\sqrt{v_f^2 + v_b^2}} + \omega O(|\varepsilon|) \text{ and } a^F = O(|\varepsilon|) \qquad (10)$$

Thus, the slow wave attenuation factor, as a function of the frequency, is of higher order than that of the fast wave.

Reflection Coefficient

Consider a plane interface between two media: one is the overburden formation and the other one is a fluid-saturated reservoir. The overburden formation is modeled as an elastic medium with density ρ_1 and compressibility β_1. For the reservoir, we adopt the poroelastic model. An incident wave arriving at the interface between the media is partially reflected and partially transmitted. Asymptotic analysis performed in the previous section can now be extended to the investigation of the dependence of the reflection coefficient on the frequency. The transmitted wave has two components: the slow one and the fast one. We will denote u_1 and u_2 the skeleton displacement in the overburden and reservoir rock, respectively. Mass and momentum conservation at the interface leads to the following boundary conditions:

$$\begin{aligned} u_1 &= u_2 \\ -\frac{1}{\beta_1}\frac{\partial u_1}{\partial x}\bigg|_{x=0} &= -\frac{1}{\beta_2}\frac{\partial u_2}{\partial x}\bigg|_{x=0} + \phi p\big|_{x=0} \\ W\big|_{x=0} &= 0 \end{aligned} \qquad (11)$$

Let U_0 be the amplitude of the incident wave. Then the total displacement in the overburden is $U_0 e^{i(\omega t - k_1 x)} + RU_0 e^{i(\omega t + k_1 x)}$, where R is the reflection coefficient. In the reservoir, the slow and fast waves have the amplitudes $T^S U_0$ and $T^F U_0$, respectively. Here T^S and T^F are transmission coefficients for the slow and fast components of the transmitted wave. Applying Equations (4), (6)-(10), for the Darcy velocity and the fluid pressure amplitude, one obtains

$$\begin{aligned} W_0^S &= -(1+\gamma_v)\,\omega T^S U^0 + \omega O(|\varepsilon|) \\ p_0^S &= \gamma_v \frac{1}{\phi\beta_f v_b}\sqrt{\frac{1}{\delta\varepsilon}}\, i\omega T^S U^0 + \omega O\left(|\varepsilon|^{1/2}\right) \end{aligned} \qquad (12)$$

and

$$\begin{aligned} W_0^F &= \omega O(|\varepsilon|) \\ p_0^F &= -\frac{1}{\phi\beta_f\sqrt{v_f^2 + v_b^2}}\, i\omega T^S U^0 + \omega O(|\varepsilon|) \end{aligned} \qquad (13)$$

Note that the assumption $\theta = O(1)$ puts the relaxation time (equivalently, the Biot's tortuosity factor) into the higher-order terms, only. Substitution of Equations (12)-(13) into the boundary conditions (11) suggests that the asymptotic expansion of the reflection coefficients have the form

$$R = R_0 + R_1\sqrt{\varepsilon} + O(\varepsilon) \qquad (14)$$

For the frequency-independent component of the reflection coefficient R_0, one obtains

$$R_0 = \frac{Z_2 - Z_1}{Z_2 + Z_1} \qquad T_0^F = \frac{2Z_2}{Z_2 + Z_1} \qquad (15)$$

where Z_1 is the acoustic impedance of the overburden formation and Z_2 is an impedance for the reservoir medium.

$$R_1 = \frac{Z_2 - Z_1}{Z_2 + Z_1}\frac{1-\delta}{1+\gamma_v} Z_3 T_0^F \qquad (16)$$

where

$$Z_3 = \frac{1-\phi}{v_b\beta_2\sqrt{\delta}} \qquad (17)$$

Frequency-dependent component of the reflection coefficient (14) is strongly affected by the rock permeability. We have used this property of the dual medium model and expression (14) for frequency-dependent seismic attribute analysis of real field data.

Field example

Here is an example of frequency-dependent seismic attribute analysis of the oil-saturated reservoir based on the Biot-Barenblatt model. The 3D seismic data were recorded using conventional acquisition technology. The data from the well logs indicate that the reservoir is 10-12 m thick, consist of sandstone, and is 3 km deep. The reservoir rock porosity varies between 0.16 and 0.18 and Core analysis shows the permeability does not exceed 100 milli-Darcy. The produced fluid composition and production rates vary from well to well. High-porosity and high-permeability material is distributed close to crest of the structure. Analysis of seismic data suggests that the wells with the highest oil production rate are located close to the fault zones. This observation implies that fractures resulting from faulting may contribute significantly to the permeability of the reservoir. The wells with the highest oil production rate (red circles) are located near the zones of the high deviation of the map of the first derivative with respect to the frequency obtained at low frequency (10 Hz). It is clear that frequency-dependent analysis at low frequency domain enhances detection of the hydrocarbons and provides information about reservoir properties. As the obtained asymptotic scaling links reservoir rock and fluid properties with seismic attributes, it has a great potential for hydrocarbon exploration and production.

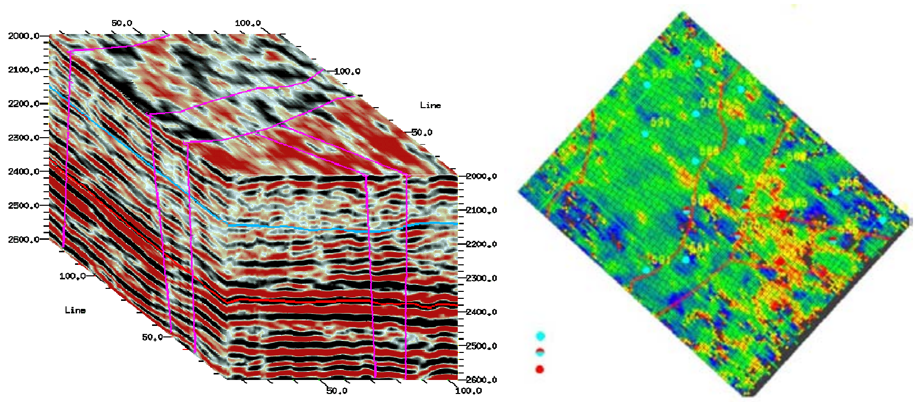

Figure 1. 3D seismic data (left) are used for frequency-dependent attribute analysis. The attribute map (right) shows the image of the first derivative (gradient) of reflected wave amplitude in frequency at low frequency (10 Hz). The map is done along reservoir surface. Red lines indicate faults and red circles show the positions of the wells with relatively high oil production rate. Anomalies of the gradient indicate oil-saturated reservoir zone with high permeability.

References

Barenblatt, G.I., Zheltov, I.P., and Kochina, I.N., 1960, Basic concepts in the theory of seepage of homogeneous liquids in fissured rocks: Journal of Applied Mathematics, v. 24, 1286-1303.
Biot, M.A., 1956a, Theory of propagation of elastic waves in a fluid-saturated porous solid. I. Low-frequency range: Journal of the Acoustical Society of America, v. 28, 168-178.
Biot, M.A., 1956b, Theory of propagation of elastic waves in a fluid-saturated porous solid. II. Higher frequency range: Journal of the Acoustical Society of America, v. 28, 179-191.
Pride, S. R. and Berryman, J. G., 2003a, Linear dynamics of double-porosity and dual-permeability materials. I. Governing equations and acoustic attenuation: Physical review. E v. 68, 036603-1-10.
Pride, S. R. and Berryman, J. G., 2003b, Linear dynamics of double-porosity and dual-permeability materials. II. Fluid transport equations: Physical review. E v. 68, 036604-1-10.
Warren J. E., and Root P. J., 1963, The behavior of naturally fractured reservoirs, SPEJ, 245–255.

Acknowledgements

This work has been performed at the University of Houston and University of California, Berkeley under Grant No. DE-FC26-04NT15503, U.S. Department of Energy.